Visual Abstract

Mechanical behaviour of sandy soils embankments treated with cement and reinforced with discrete elements (fibres)

Mohamed Bouteben Yasmine, Boudaoud Zeineddine
Faculty of science and applied sciences, Department of Civil Engineering, Larbi Ben M'hidi University, Oum El Bouaghi, Algeria.
medboutebenyasmine@outlook.fr, zboudaoud@yahoo.fr

ABSTRACT. It is well known that chemical treatment with cement and reinforcement with polypropylene fibres are considered as a solution to soil stability problems. This technique ameliorates the mechanical and physical comportment of the soil. Based on this, this research paper aims at investigating the mechanical behaviour of a specific type of dried-cemented-sandy soil reinforced with discrete elements such as polypropylene fibre basically through experimental tests. The latter is a series of consolidated drained triaxial tests which were carried out on sand samples that are prepared with 0, 3 and 6% of cement, reinforced with 1% of polypropylene fibre (12, 18 mm) randomly distributed. Furthermore, those contents are measured by the volume of dry sand. In addition to these tests, the mechanical properties of two types of reinforced sand obtained experimentally, were used in a numerical analysis of a road embankment using a finite element program such as Plaxis 2D in order to observe the variation of different parameters like safety factor and the displacements (Ut, Ux, Uy). The test results showed that the addition of cement and polypropylene fibre of different accommodations increased both cohesion and friction angle of sands while the numerical results indicated that the presence of these additions improved the safety factor and decreased significantly the displacements.

KEYWORDS. Sand; Triaxial; Polypropylene Fibre; Cement; Cohesion; Friction Angle.

OPEN ACCESS

Citation: Yasmine, M. B., Zeineddine, BMechanical behaviour of sandy soils embankments treated with cement and reinforced with discrete elements (fibres), Frattura ed Integrità Strutturale, 60 (2022) 174-186.

Received: 05.12.2021
Accepted: 28.01.2022
Online first: 31.01.2022
Published: 01.04.2022

INTRODUCTION

As a result, of the noticeable demographic expansion and the different infrastructural causes are sometimes inevitable to build on an unsatisfactory Geotechnical site. On this basis the improvement of the mechanical characteristics of this site is required. Consequently, different techniques can be considered, namely: drainage, densification, cementation, strengthening, drying, and heat treatment. Those techniques have been part of soil development for a long time. Cement and fibre improvement have become a well-known and widely utilised methodology in Geotechnics. Fibres improved the soil's physical characteristics and increased its ability to support the charges. Cement stabilisation, on the other hand, made the soil more resistant to climate influences.

The act of including cement with various amounts in the reinforced sand displayed that it acts fragile due to the increase in the compression strength [1]. Additionally, the researchers discovered that the nature and length of the fibre had an impact on the yield matrix of fibre, cement, sand, and they found that the polypropylene fibres improved their mechanical behaviour and reduced the beach sand dilation [2-4]. Hamed et al [5], also tested sand specimens reinforced with glass and polypropylene fibres under varied confining pressures and relative densities in a series of monotonic triaxial tests. The results showed that fibres improved shear strength by increasing confinement and relative density. Hence, the features of bio-cemented sand improved greatly after the addition of fibres and the rise of strength was larger when polypropylene fibres were present. A series of compression tests, tensile tests as well as calcium carbonate content tests were conducted to investigate the impact of different fibres on bio cemented sand. According to the findings the presence of inclusions converted the fragile failure mode to ductile, the non-confined compression resistance, improved and increased as the fibre concentration increased, but it dropped when polypropylene fibre percentage exceeded 0.2% (This drop resulted in the fibre's low elastic modulus) [6,7]. Furthermore, the polypropylene fibre produced more residual resistance throughout the curing process. Dry density, permeability, non-confined compressive strength (UCS), tensile strength, and microstructure were measured to see how fibre addition, affected the characteristics of treated sand with calcium carbonate precipitation (MICP) created by scanning electron microscopy (SEM). The MICP-treated sand had a lower permeability, a higher dry density, and a lower confined compression resistance; however, the addition of fibre improved ductility, mode of failure, traction resistance, and dry density. The features of the treated sand were influenced by the length of the fibres as well as the fibre concentration [8]. On the other hand, a numerical modelling is one of the most widely used simulation approaches in civil engineering, notably in Geotechnical engineering. It was constructed in order to obtain a comprehensive description of soil behaviour. Skuodis et al [9], employed a Plaxis 3D model to evaluate the damage produced to the geogrid during triaxial tests performed on reinforced sand samples, this model offered a clear explanation of the major cause of the damage by analysing numerical and experimental results. Ver H. Abioghli and A. Hamidi [10], developed a constitutive model of generalised plasticity to predict the mechanical behaviour of sand reinforced with cement and fibre; as a result, the soil behaviour was well characterised by this model.

The main aim of this research paper is to work on sandy soil (from two different regions) reinforced with fibre and cement, using 1% PP fibres (12, 18 mm) randomly distributed and 0, 3 and 6% cement. The first portion depicts the samples' mechanical behaviour in triaxial tests, while the second part is a parametric analysis on a road embankment with and without reinforcing using a finite element program and based on the experimental results.

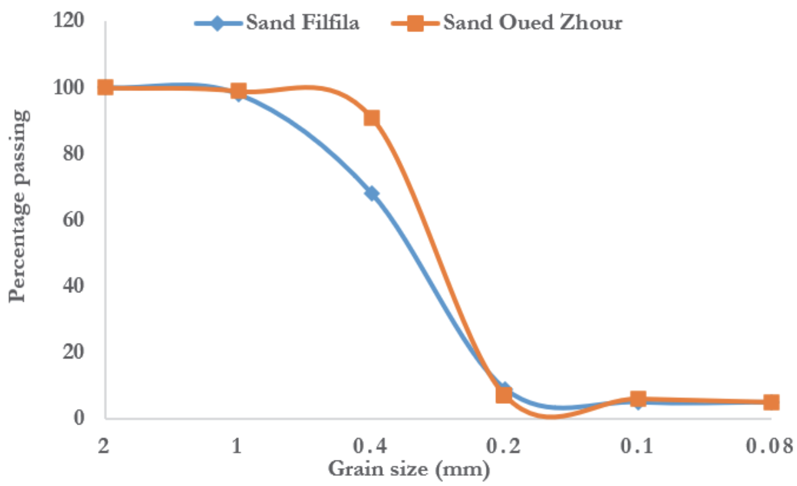

Figure 1: Grain size distribution curves for the sands

EXPERIMENTAL

The materials used and tested in this study are two dune grains of sand from Algeria, Skikda (Oued Zhour and Filfila).

- The sand of Oued Zhour (S1) had a density estimated at 1.62 g/cm³ with a uniformity coefficient Cu and curvature coefficient Cc of 1.5 and 0.93 respectively.
- The sand of Filfila (S2) showed 1.65 g/cm³ of density with Cu and Cc of 1.03 and 1.9 respectively.

Fig. 1 demonstrates the gradation of these sands while Tab. 1 presents their structures.

Physical property	Value (Oued Zhour sand)	Value (Filfila sand)
Particle size such that 50% are smaller, D50 (mm)	0.35	0.38
Particle size such that 10% are smaller, D10 (mm)	0.22	0.2
Coefficient of uniformity, Cu	1.5	1.03
Coefficient of curvature, Cc	0.93	1.9
density (g/cm^3)	1.62	1.65
Particle size such that 50% are smaller, D50 (mm)	0.35	0.38

Table 1: Physical properties of sands.

The experiments were started on sand treated, with cement Portland type II (0, 3 and 6%) made by an Algerian cement company which contains 2.28% residues, 2.41% insoluble, 57.22% PAF $_{975}$, 27.83% CaO, 3.12% Fe_3O_3, 0.94% MgO, 2.02% SO_3, and 0.88% CaO free. Then reinforced with 1% discrete components (12 and 18 mm) randomly distributed which has a circular section, 32 microns thickness, 0.8-1.00 g/cm^3 density, 0,91 g/cm^3 specific weight, 160° fusion point and two lengths (12, 18 mm). The characteristics of these elements are shown in Tab. 2 while the Tab. 3 shows the different components and its abbreviation. The experimental work includes the preparation of the samples and the triaxial shears (CD). 42 samples have been consolidated for 15 days under a cell pressure (CP) 50, 100 and 200 kPa. Fig. 2 presents the triaxial machine used in this work also Fig. 3 shows the specimen before and after shearing. The purpose of this study is investigating the effect of cement and the addition of PP fibre on those sands of the two different regions.

Physical property	Fibres
Material	Polypropylene virgin
Colour	Natural white
Density	0.8 à 1.00 g/cm^3
Dimension	6 mm
Length	12/18 mm
Section	Circular
Thickness	32 microns
Specific weight	0.91 g/cm^3
Fusion point	160°

Table 2. Physical properties of the polypropylene fibres used.

CC (%)	FL (mm)	Abbreviation
0	0	0%C+0F
3	0	3%C
	12	3%C+F12
	18	3%C+F18
6	0	6%C
	12	6%C+F12
	18	6%C+F18

Table 3: The proportion of cement and fibre.

Figure 2: Triaxial machine.

a) Before shears. b) After shears.

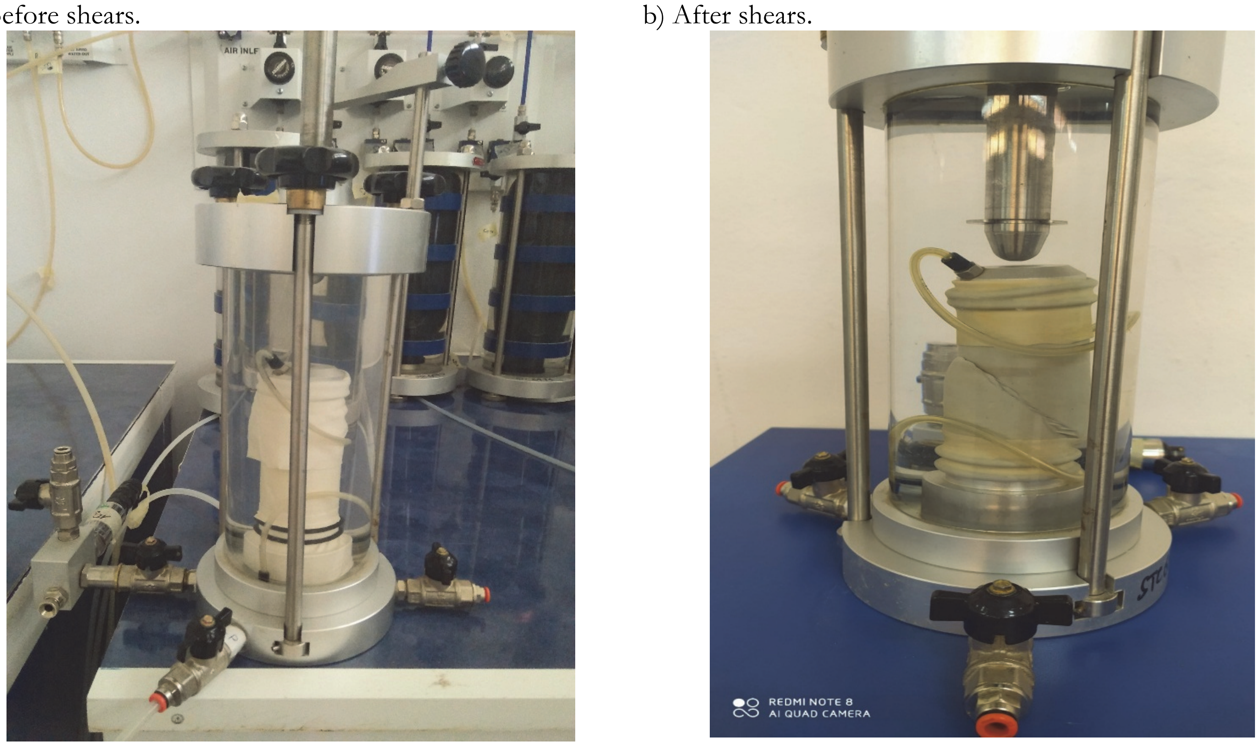

Figure 3: Sand specimen before and after performing the shear test.

Triaxial test procedure

The procedure followed in this test is mixing the cement and fibre contents of the samples calculated from the volume of dry sand by hand (ordinary method) until the distribution of fibres is achieved. Each sample is made up of five layers of mixed components, each weighing 125g. Then it is encased in a silicone membrane (38 mm diameter and 70 mm long). The layers are compacted slightly, then saturated, consolidated and sheared on triaxial. The test compression program (CD) has the following steps.

1- The preparation of the samples.

2- Applying a negative pressure to make the sample stable.

3- Injecting water into the specimen through the bottom drainage line to remove the air from the specimen by flushing it out.
4- Saturating the samples by increasing cell pressure gradually, once the Skempton pore pressure parameter β exceeds by 95%.

$$\beta = \Delta u / \Delta\sigma_3 \text{ is} > 95\ \% \qquad (1)$$

β : Skempton pore pressure parameter.
Δu : The resultant change in pore pressure obtained under the undrained isotropic compression condition.
$\Delta\sigma_3$: The isotropic cell pressure.
5- The consolidation of the samples under CP 50, 100, 200 KPa. When the volume variation reaches constant values, the consolidation is complete.
6- Under draining circumstances with an axial displacement rate of 1 mm/min, shear loading is given with regard to a constant confining pressure to specimen failure [11-13].

Results and discussion of triaxial compression test

Tab. 4 shows the main characteristics of the tests (deviator stress, confining pressure, and axial strain). While Figs. 4, 5 and 6 illustrate the deviator stress as a function of axial strain for sand, cemented sand, and fibre cemented sand samples under various confining pressures (50, 100, 200 kPa). Furthermore, Fig. 4 shows the variation between deviator stress and axial strain in S1 (continuous line) and S2 (discontinuous line) at a confining pressure of around 50 kPa. Figs. 5 and 6 demonstrate the evolution of deviator stress with axial strain for S1 and S2 sheared at effective stress σ'c = 100 and 200 kPa respectively. It appears in Figs. 4, 5 and 6 that the deviator stress increases with the increase of axial strain until a maximum value than it drops after the failure.

CC (%)	FL (mm)	CP (kPa)	Deviator Stress (kPa)		Axial Strain (%)	
			S1	S2	S1	S2
0	0	50	0.13	0.12	5.61	6.57
0	0	100	0.31	0.21	4.74	2.8
0	0	200	0.5	0.51	6.51	5.63
3	0	50	2.34	0.21	4.42	4.23
3	0	100	4.19	0.39	6.51	9.11
3	0	200	6.09	0.62	9.06	10.69
3	12	50	0.43	0.42	5.75	6.39
3	12	100	0.8	0.82	6.30	4.09
3	12	200	1 .02	0.96	11.02	12.61
3	18	50	0.7	0.61	12.57	13.67
3	18	100	0.93	0.87	12.27	17.99
3	18	200	1.5	1.38	7.40	11.26
6	0	50	2.92	3.23	5.04	4.64
6	0	100	4.35	4.16	12.97	15.73
6	0	200	6.83	7.28	11.06	12.80
6	12	50	0.77	0.76	7.69	4.37
6	12	100	0.92	0.89	5.54	5.66
6	12	200	1.58	1.52	4.39	4.21
6	18	50	0.81	0.79	1.72	5.18
6	18	100	1.46	1.14	9.91	12.46
6	18	200	1.59	1.6	7.23	13.43

Table 4: Summary of triaxial tests results.

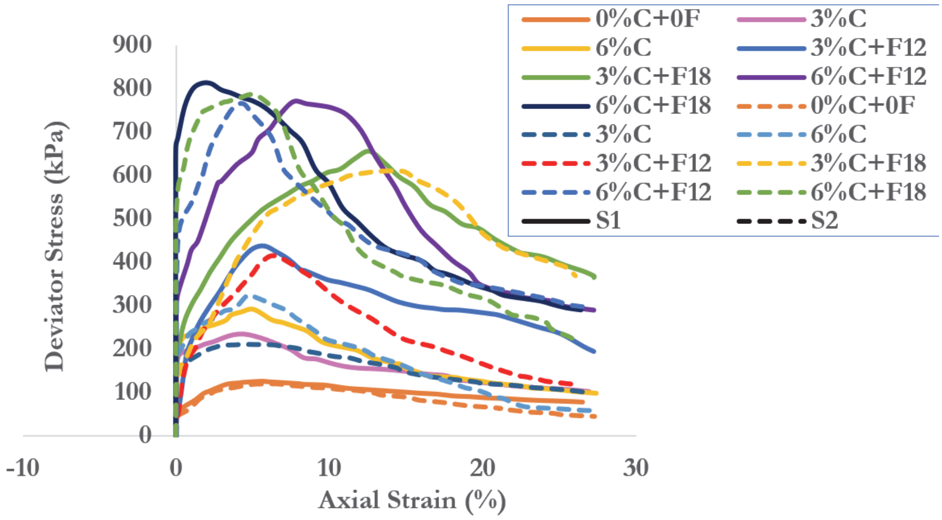

Figure 4: Stress-strain behaviour of S1 and S2 samples with CP=50 kPa.

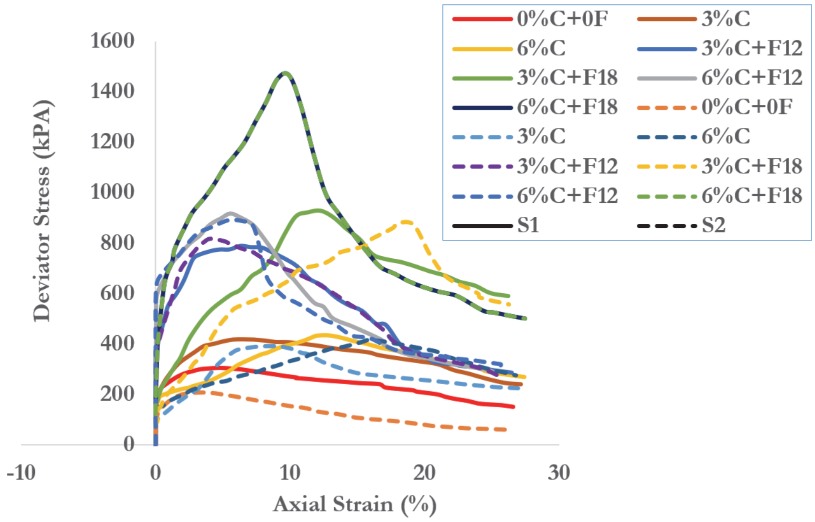

Figure 5: Stress-strain behaviour of S1 and S2 samples with CP=100 kPa.

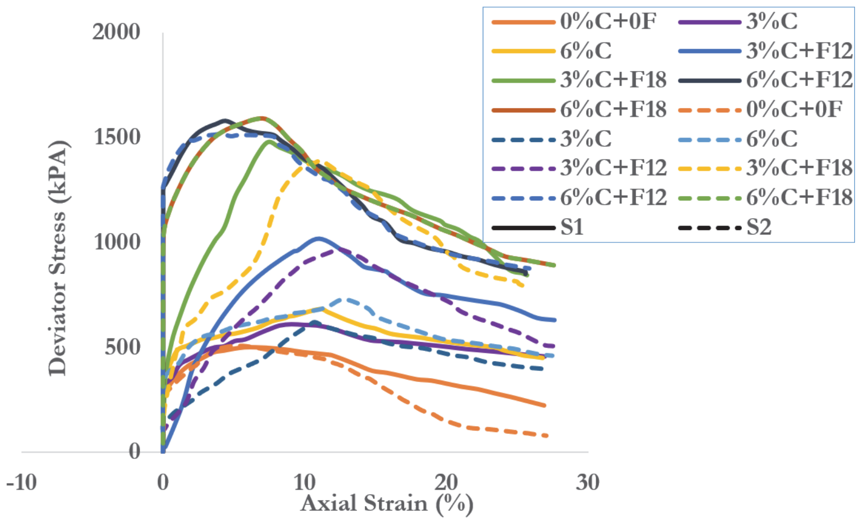

Figure 6: Stress-strain behaviour of S1 and S2 samples with CP=200 kPa.

It is clearly seen in Tab. 5 and Figs. (7, 8) that the inclusion of cement and fibre improve the cohesiveness and friction angle of both of these grains of sand. We can see that the cohesion is increasing gradually from 5.81 to 57.75 and from 6.97 to 59.59 in S1, S2 respectively. As well the friction angle goes from 33.31, 34.81 to 47.70, 46.55 in S1, S2 respectively. Several studies have demonstrated that this improvement ameliorated the mechanical characteristics of the soil. Furthermore, according to this study [14], one of the most important elements affecting the strength of sandy soil compression was the cement content; while the introduction of the PP fibre into the soil in order to evaluate its behaviour showed that it was a reinforcing ingredient in the soil particle binding [15]. As well the results of other experiments which were done by M.M. Benziane et al [16], demonstrated that the inclusion and the increase of PP fibre improved the mechanical properties of the sandy soil. Additionally, researchers confirmed that Fibres have a significant impact on the mechanical performance of fibre-reinforced cement treated sand (CTSF) utilised for road and pavement applications [17]. Moreover, the presence of cement simply reduced the deviator stress, according to triaxial testing, as well as the addition of fibre to cemented sand enhances this deviator stress (Fig. 4, 5 and 6). The failure is observed with the peak value. After failing, it decreases to a constant value. It has been discovered that ground strength with fibre had exhibited high strength, resulting in an increase in compression resistance and a considerable improvement in sand behaviour. Because of its flexible shape and force qualities, the polypropylene fibre provided better ground resistance [18]. Juan Du et al said that Cement soil stabilisation necessitated a high confinement pressure as well as a prolonged hard time. As confinement pressure rose, so did the tension of the deviator [19].

Cement content (%)	Fibre length (mm)	C' (kPa)		Φ' °	
		S1	S2	S1	S2
0	0	5.81	6.97	33.31	34.81
3	0	29.95	20.4	33.44	34.9
3	12	50.23	48.4	41.13	40.81
3	18	50.78	49.76	47.14	46.1
6	0	36.46	35.24	34.38	35.43
6	12	53.31	59.99	47.70	46.55
6	18	57.75	76.18	47.87	46.71

Table 5: Peak strength parameters for sands and fibre-reinforced cemented sands.

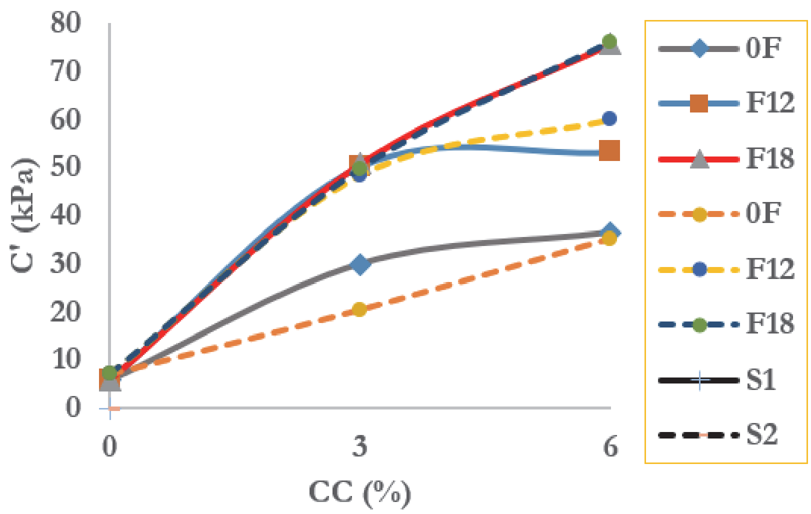

Figure 7: Variation of cohesion in presence of components for S1 and S2.

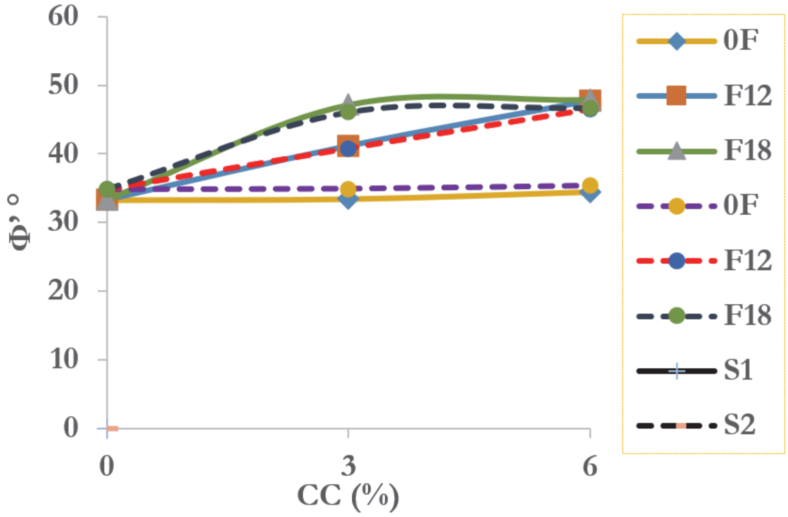

Figure 8: Variation of friction angle in presence of components for S1 and S2.

Moreover, Fig. 9 represents the amelioration of deviator stress with the increase of the confining pressure. The test results show that the cement percentage and fibre length increase as the strength increases. These observations are shown in both S1 and S2. In conclusion, the figures clearly confirm that the deviator stress increases as cement content, fibre length and confining pressure. These ameliorations are confirmed by researchers where they improved the soil reinforcement with PP fibre, however the cohesion and shear resistance of sand improved significantly as fibre content and length increased [20]. Also in addition to this, the increase in the length of fibre has increased the ground compression indices so fibre have an impact on soil behaviour [21].

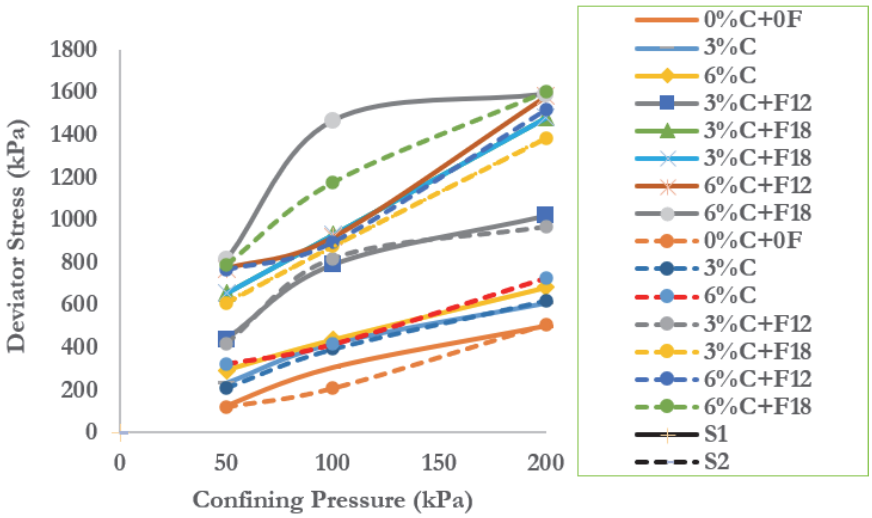

Figure 9: Variation of deviator stress with different confining pressures of S1 and S2.

Numerical modelling

This study investigates the stability of a road embankment using the finite element method of Plaxis 2D. This analysis was performed by using the results of the experimental tests. The model present in this study is 80m long and 10m high, the road embankment is 4 m high on top of two layers of foundation clay with varied characteristics, each layer is 3 m high. The studied variable is simulated on half of it because it is symmetrical as the Fig. 10 shows. The Mohr-Coulomb (MC) model was used to analyse the road embankment (with and without reinforcement) in a drained condition, whereas the examination of the foundation clay soil was done in an undrained situation [22]. The MC model is a well-known, widely utilised today and is an initial estimate of soil behaviour in Plaxis [23]. The 2D Plaxis model was used to simulate the investigation of an in-depth tunnel excavation by the MC model. Following this examination, the researchers discovered that as the tunnel's depth climbs, the colonies on the soil's surface shrink and approach their true values [24]. On the other hand, the excavation has increased again because of the unloading behaviour (softer or weaker) and the stiffness parameter that minimises deformation. [25]. Two different sequences-modelling methodologies were used in this investigation. The stability of an unreinforced road has been investigated for the first time and the stability of the reinforced embankment model was then evaluated using various cement props and fibre lengths. The material parameters of the two sands embankments and the road foundation clays are shown in Tab. 6. Although Figs. 11 and 12 depict the road's deformation before and after strengthening.

A road embankment is achieved to calculate the safety factor, to observe displacement changes (total, horizontal and vertical) with and without reinforcing. The following steps have been used in the simulation of the problem:

- Model creation;
- The input of material parameter and a simple finite element mesh may be generated;
- Consolidation phase to allow the excess pore pressure and analysis the ultimate time required;
- Characteristics computation (safety factor, the displacements).

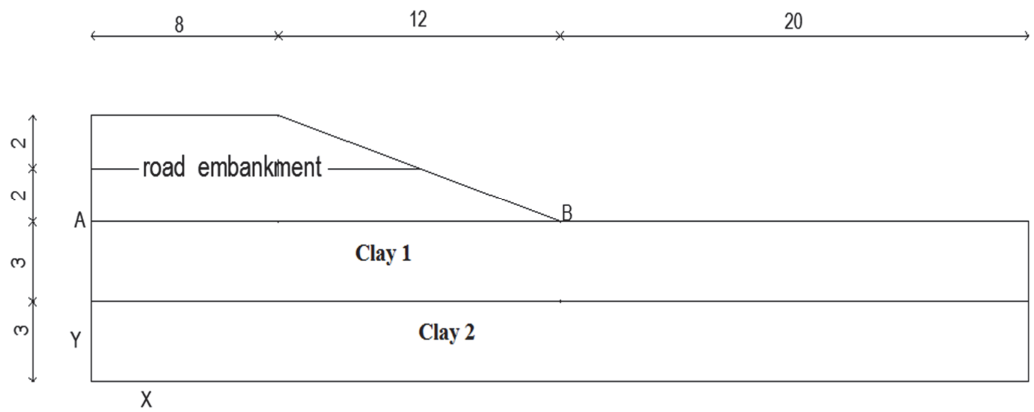

Figure 10: Geometry model of road embankment.

Parameter	Name	Clay 1	Clay 2	Embankment S1	Embankment S2	Unit
Material model	Model	MC	MC	MC	MC	-
Type of drainage	Type	undrained	undrained	drained	drained	-
Soil unit weight above phreatic level	γ_{unsat}	16.6	16.6	18	16	kN/m³
Soil unit weight below phreatic level	γ_{sat}	17.31	17.31	22	21	kN/m³
Young's ratio	E_{ref}	2000	2000	2200	1500	kN/m²
Cohesion	C'	33.02	12.01	5.81	6.97	kN/m²
Friction angle	Φ'	1	1	33.31	34.81	°
Dilatancy angle	Ψ	0.0	0.0	3.31	4.81	°

Table 6: Material properties used in finite element analysis.

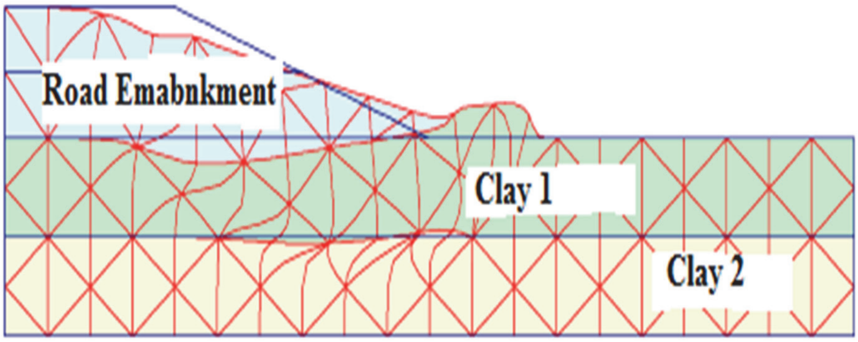

Figure 11: Material Deformation mech of the road before reinforcement.

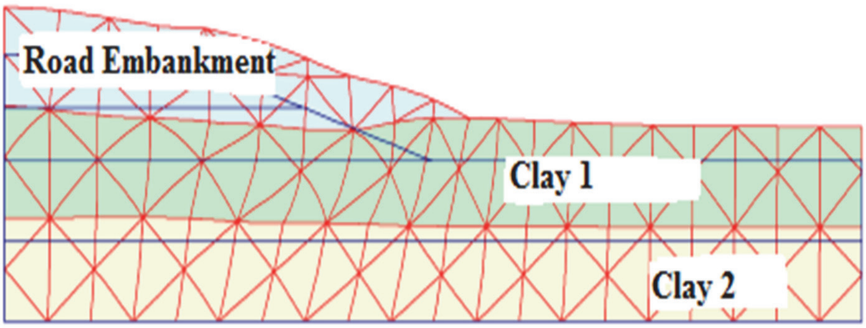

Figure 12: Material Deformation mech of the road after reinforcement.

Results of the numerical modelling and discussion

Tab. 7 and Figs. (13-16) show the results of the numerical modelling. The safety factor increases as cement content and fibre lengthens. It goes from 1.38, 1.5 to 1.68, 1.8 in S1, S2 respectively. Sandbox 1 and 2 displacements variations reduce as cement and fibre length increase until they reach a minimal value then they increase significantly. These results were confirmed in previous studies. The stability of a roadway slope was explored using the 2D Plaxis to model the light weight of the embankment. The simulation revealed that employing Geogrids as a reinforcing material improved the security factor [26], as well a study of a road embankment reinforced by Geotextiles showed that the safety factor increased as the Geotextile's tensile strength increased, while the displacements dropped [22].

In order to validate the existing model, the findings of the current investigation were compared to the data reported by P.S. Wulandari and D. Tjandra [22]. Based on the test model the road embankment stability was assessed using the finite element approach in Plaxis 2D. As a basic preliminary examination of the problem, the Mohr-Coulomb model was applied. According to the findings, level of the tensile strength of Geotextile reinforcement tend to raise the factor of safety while the displacement along the embankment's base is reduced by the increasing Geotextile tensile strength [22].

Abbreviation	SF		Ux (cm)		Uy (cm)		Ut (cm)	
	S1	S2	S1	S2	S1	S2	S1	S2
0%C+0F	1.38	1.5	3.18	2.69	2.1	2.38	3.33	3.26
3%C	1.64	1.69	2.79	2.70	2.12	2.39	2.99	3.03
3%C+F12	1.67	1.8	2.79	2.68	2.13	2.43	2.98	2.99
3%C+F18	1.68	1.8	2.77	2.70	2.12	2.33	2.96	3.01
6%C	1.66	1.78	2.79	2.69	2.12	2.33	2.98	3.02
6%C+F12	1.68	1.79	2.80	2.67	2.13	2.39	3.04	3.0
6%C+F18	1.68	1.8	2.79	2.68	2.11	2.37	3.01	2.99

Table 7: Numeric model results.

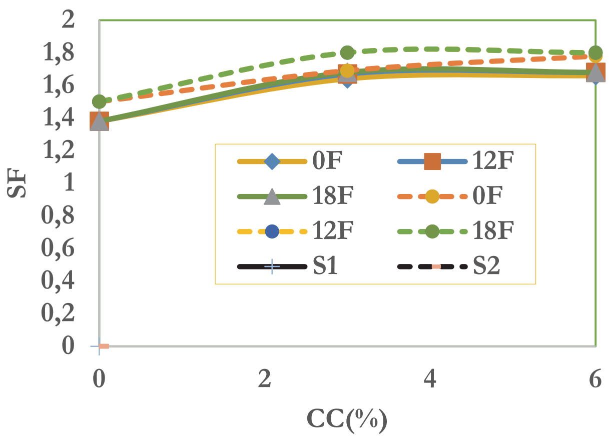

Figure 13: Safety factor analysis of S1 and S2.

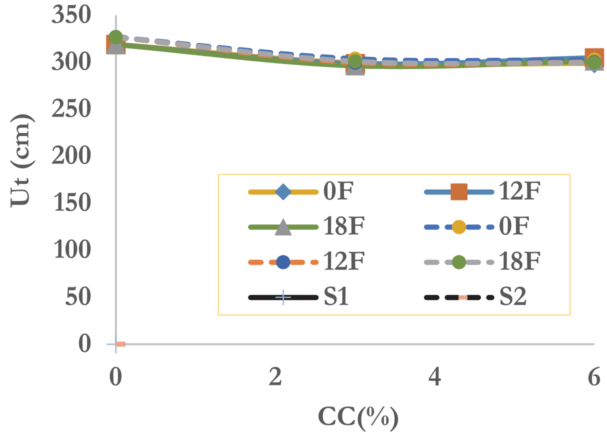

Figure 14: Variation of Total Displacement of S1 and S2.

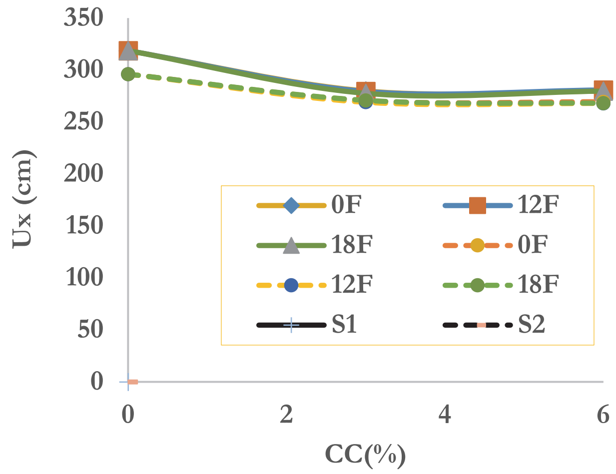

Figure 15: Variation of Horizontal Displacement of S1 and S2.

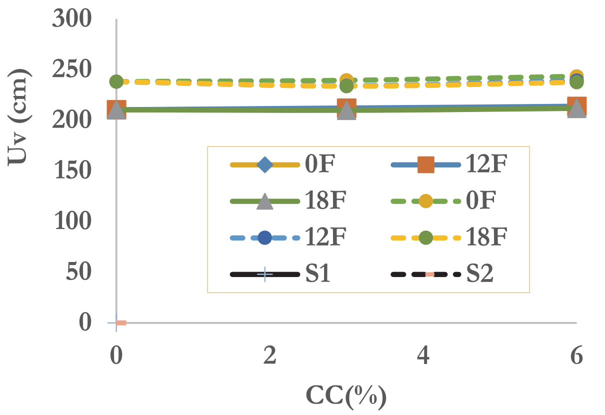

Figure 16: Variation of Vertical Displacement of S1 and S2.

CONCLUSION

After studying the impact of cement and fibre on the behaviour of two dune sand grains in addition to conducting the parametric study using Plaxis 2D which was used to assess the stability of the road embankment. On this basis, the results of this analysis are outlined as follows:

- The addition of cement and fibre improved the sand's properties.
- The cohesion and the fraction angle increased exponentially with cement and fibre length.
- Deviator stress, increased exponentially with cement, fibre length, and confining pressure.
- The increase in safety factor indicates the stability of the road embankment.
- The cement and fibre enhanced the safety factor until it reached a needed value, whilst the displacements (total, vertical and horizontal) dropped to a minimal value, then rose.
- When comparing the results, we find that the two studied sands have the same behaviour.

Data Availability

The author did the experimental results and the Geotechnical analysis of sandy soil (Skikda city) himself, and the produced numerical model, which supports the conclusions in this work, is accessible upon request from the corresponding author.

PERSPECTIVES

Reinforcement is a well-known approach nowadays. The availability of fibre and cement has shown to be a solution in the laboratory for improving soil behaviour. Furthermore, the influence of additions on soil, ground characteristics (safety factor, displacements) may be numerically investigated.

Abbreviations

The following abbreviations are used in this paper:
Cement content (CC).
Fibre Length (FL).
Oued Zour Sand (S1) with continuous line.
Filfila Sand (S2) with discontinuous line.
Polypropylene (PP).
Consolidated drained (CD).
Cell pressure (CP).
Mohr Coulomb Model (MC).
The total displacement (Ut).
The displacements in direction x, y (Ux), (Uy).
3% C+F12 means: 3% of cement, 1% of fibre length (12 mm).
3%C means 3% of cement.
0F means 0% fibre.

References

[1] Raja, K., Elakkya, E., Manikandan, A.T., Surya, B., Nekila, M. (2021). Strength characteristics developed in cement stabilized soil, IOP Conf. Ser. Mater. Sci. Eng., 1055(1), pp. 012039, DOI: 10.1088/1757-899X/1055/1/012039.
[2] Jamsawang, P., Suansomjeen, T., Sukontasukkul, P., Jongpradist, P., Bergado, D.T. (2018). Comparative flexural performance of compacted cement-fiber-sand, Geotext. Geomembranes, 46(4), pp. 414–425, DOI: 10.1016/j.geotexmem.2018.03.008.
[3] Lv, X., Yang, X., Zhou, H., Zhang, S. (2019). Mechanical behavior of cemented sand reinforced with different polymer fibers, Adv. Mater. Sci. Eng., 2019, DOI: 10.1155/2019/8649619.
[4] Kodicherla, S.P.K., Muktinuthalapati, J., Revanna, N. (2018). Effect of randomly distributed fibre reinforcements on engineering properties of beach sand, Jordan J. Civ. Eng., 12(1).
[5] Javdanian, H., Soltani, N., Shams, G., Ghorbani, S. (2021). Investigating the monotonic behavior of fiber-reinforced soil under triaxial compression using experimental modeling, Model. Earth Syst. Environ., 7(2), pp. 943–952, DOI: 10.1007/s40808-020-00920-9.
[6] Lv, C., Zhu, C., Tang, C.-S., Cheng, Q., Yin, L.-Y., Shi, B. (2021). Effect of fiber reinforcement on the mechanical behavior of bio-cemented sand, Geosynth. Int., 28(2), pp. 195–205, DOI: 10.1680/jgein.20.00037.
[7] Lei, X., Lin, S., Meng, Q., Liao, X., Xu, J. (2020). Influence of different fiber types on properties of biocemented calcareous sand, Arab. J. Geosci., 13(8), pp. 317, DOI: 10.1007/s12517-020-05309-7.
[8] Fang, X., Yang, Y., Chen, Z., Liu, H., Xiao, Y., Shen, C. (2020). Influence of Fiber Content and Length on Engineering Properties of MICP-Treated Coral Sand, Geomicrobiol. J., 37(6), pp. 582–594, DOI: 10.1080/01490451.2020.1743392.

[9] Skuodis, Š., Dirgėlienė, N., Medzvieckas, J. (2020). Using Triaxial Tests to Determine the Shearing Strength of Geogrid-Reinforced Sand, Stud. Geotech. Mech., 42(4), pp. 341–354, DOI: 10.2478/sgem-2020-0005.
[10] Abioghli, H., Hamidi, A. (2019). A constitutive model for evaluation of mechanical behavior of fiber-reinforced cemented sand, J. Rock Mech. Geotech. Eng., 11(2), pp. 349–360, DOI: 10.1016/j.jrmge.2018.11.003.
[11] ASTM. (2011). Method for consolidated drained triaxial compression test for soils, D 7181, Annu. B. Stand.
[12] Lade, P. V. (2016). Triaxial Testing of Soils, John Wiley & Sons, Ltd.
[13] Souadeuk, A., Boudaoud, Z. (2022). Reinforced Soft Soil by CSV with/without Polypropylene fibres: Experimental and Numerical analysis., Frat. Ed Integrità Strutt., 16(59), pp. 374–395, DOI: 10.3221/IGF-ESIS.59.25.
[14] Geng, J., Chen, M., Shang, T., Xue, C., Chen, H., Zhang, C. (2021). The Influence of an Expansive Agent on the Performance of Cement-Stabilized Coral Sand, Adv. Civ. Eng., 2021, pp. 1–10, DOI: 10.1155/2021/8830070.
[15] Tomar, A., Sharma, T., Singh, S. (2020). Strength properties and durability of clay soil treated with mixture of nano silica and Polypropylene fiber, Mater. Today Proc., 26, pp. 3449–3457, DOI: 10.1016/j.matpr.2019.12.239.
[16] Benziane, M.M., Della, N., Denine, S., Sert, S., Nouri, S. (2019). Effect of randomly distributed polypropylene fiber reinforcement on the shear behavior of sandy soil, Stud. Geotech. Mech., 41(3), pp. 151–159, DOI: 10.2478/sgem-2019-0014.
[17] Chindaprasirt, P., Jamsawang, P., Sukontasukkul, P., Jongpradist, P., Likitlersuang, S. (2021). Comparative mechanical performances of cement-treated sand reinforced with fiber for road and pavement applications, Transp. Geotech., 30, pp. 100626, DOI: 10.1016/j.trgeo.2021.100626.
[18] Liu, J., Bai, Y., Song, Z., Kanungo, D.P., Wang, Y., Bu, F., Chen, Z., Shi, X. (2020). Stabilization of sand using different types of short fibers and organic polymer, Constr. Build. Mater., 253, pp. 119164, DOI: 10.1016/j.conbuildmat.2020.119164.
[19] Du, J., Zheng, G., Liu, B., Jiang, N.-J., Hu, J. (2021). Triaxial behavior of cement-stabilized organic matter–disseminated sand, Acta Geotech., 16(1), pp. 211–220, DOI: 10.1007/s11440-020-00992-y.
[20] Bao, X., Li, L., Liao, Z., Cui, H., Tang, W., Chen, X. (2021). Study of silty sand slope protection from seepage flows using short fiber-sand mixtures, Geosynth. Int., 28(5), pp. 491–507, DOI: 10.1680/jgein.21.00028.
[21] Al-Mahbashi, A.M., Al-Shamrani, M.A., Moghal, A.A.B. (2020). Soil–Water Characteristic Curve and One-Dimensional Deformation Characteristics of Fiber-Reinforced Lime-Blended Expansive Soil, J. Mater. Civ. Eng., 32(6), pp. 04020125, DOI: 10.1061/(ASCE)MT.1943-5533.0003204.
[22] Wulandari, P.S., Tjandra, D. (2015). Analysis of Geotextile Reinforced Road Embankment Using PLAXIS 2D, Procedia Eng., 125, pp. 358–362, DOI: 10.1016/j.proeng.2015.11.075.
[23] Tran, T.N.D., Ahmed, Z., Nguyen, Q.B. (n.d.). Application of plaxis for calculating the construction stability and soft embankment in protecting Ha Thanh river, Binh Dinh Province, 2nd Conference on Sustainability in Civil Engineering (CSCE'20), Department of Civil Engineering Capital University of Science and Technology, Islamabad Pakistan.
[24] Çelik, S. (2017). Comparison of mohr-coulomb and hardening soil models' numerical estimation of ground surface settlement caused by tunneling, Iğdır Univ. J. Inst. Sci. Technol., 7(4), pp. 95–102.
[25] Gaur, A., Sahay, A. (2017). Comparison of different soil models for excavation using retaining walls, SSRG Int. J. Civ. Eng., 4(3), pp. 43–48.
[26] Khan, S.A., Abbas, S.M. (2014). Numerical modelling of highway embankment by different ground improvement techniques, Int. J. Innov. Res. Adv. Eng., 1(10), pp. 350–356.